July 1998, revised December 1998 ULG-PNT-98-2-JRC

FERMI MOTION AND QUARK OFF-SHELLNESS IN ELASTIC VECTOR MESON PRODUCTION

Isabelle Royen[1] and Jean-René Cudell[2]
Inst. de Physique, U. de Liège, Bât. B-5, Sart Tilman, B4000 Liège, Belgium

Abstract

We study ways of implementing Fermi momentum in elastic vector-meson production, and find that the usual on-shell assumption of quark models and quark wave functions cannot reproduce the ratio σ_L/σ_T. We propose a new approach which allows the quarks to be off-shell, and which naturally reproduces the data. As a consequence, we prove that the asymptotic form of the transverse cross section is different from $\sigma_T \sim 1/Q^8$. In this new model, we show that the mass, t and Q^2 dependence of the cross sections are also reproduced. We also make predictions concerning the production of excited states such as the ρ' and the ψ'.

PACS numbers: 13.20.Cz, 13.60.Le, 14.65.Bt
Keywords: quasielastic electroproduction of mesons, quark model, quark wave functions, transverse cross section.

[1]iroyen@ulg.ac.be
[2]JR.Cudell@ulg.ac.be

1 Introduction

The data from HERA have now reached a remarkable level of accuracy, and in particular they provide us with excellent information on vector meson elastic production [1, 2]. We have precise measurements of the photon Q^2, t and w^2 dependences of the cross section, for different mesons, as well as information on its transverse and longitudinal components, Q^2 being the absolute value of the photon off-shellness, t the square of the momentum transferred to the proton and w^2 the square of the center-of-mass energy of the $\gamma^{(*)}p$ process.

Theoretically, this is related to a measurement of the off-diagonal deep-inelastic tensor $W^{\mu\nu}(x, Q^2, m_V^2, t)$, for t non zero. One may hope that the presence of two new scales - the vector meson mass m_V and the momentum transfer t would enable one to concentrate on regions where the perturbative calculation is reliable, and observe how one can extend it to smaller scales. Theoretically, these studies have recently been set on a firm ground as Collins, Frankfurt and Strikman [3] have shown that a factorisation theorem exists for exclusive vector meson production. This theorem asserts that, to leading power of Q^2 and to all logarithms, the cross section is the convolution in longitudinal momentum of a hard scattering amplitude, an off-diagonal structure function and a meson wave function. Furthermore, the theorem can be proven irrespectively of the meson mass. Hence at high Q^2, even light meson production can be reliably calculated.

The w^2 dependence of the cross section then results from the x, t/w^2 and m_V^2/w^2 dependence of these new distribution functions. It is to be noted that these are new objects which are different from the diagonal structure functions. Also, the theorem naturally holds for longitudinal vector meson production, which is leading in Q^2, and for which one can show that the off-shell distributions are related to the usual gluon distribution. The transverse cross section σ_T is *a priori* down by a factor Q^2. However, the factorisation theorem envisions the possibility of a different behaviour, but the price to pay, in the case of massless quarks, is to allow the leading behaviour of σ_T to come totally from the non-perturbative region, for quark off-shellnesses of order m_V^4/Q^2. In this paper, we shall go beyond this analysis by including massive quarks in a model describing the transition from a photon to a QCD bound state. One indeed needs to disentangle the effect of this transition on the transverse cross section, before one can extract the off-diagonal distributions accurately.

One expects (and we confirm) that the transition $\gamma^* \to V$ will not modify the w^2 dependence significantly at high energy. The w^2 dependence is surely one of the outstanding problems of QCD, and our theoretical understanding of it seems to have made a big step recently [4], although it is difficult to assert yet in which direction. We shall make the simplifying assumption that it enters as a constant factor which does not depend on any variable but t. We shall come back later to the significance of this assumption.

We could of course, as often done nowadays, assume that this factor is related to $W(t=0)$ and is proportional to $[xg(x)]^2$. However, we want first to point out that this correspondence exists only for longitudinal cross sections, and is only approximate. Indeed, as we shall explain below, the imbalance between initial and final states in vector-meson elastic production brings one to a different kinematic domain from DIS. This has important consequences for quantities related to the upper loop of a ladder, especially in the transverse case.

Hence we shall simply calculate up to a factor, and we shall not claim that we can reliably predict it. On the other hand, the Q^2 and m_V dependences mainly (up to logarithms) come from the upper loop. As we shall see, the data is not precise enough (or Q^2 not large enough) to require the inclusion of evolution effects. As for the t dependence, it comes from the proton form factor, the $\gamma^* V$ loop, and W. We shall show here that simple assumptions enable one to reproduce the data at small t, and that high-t points do not seem to require either a pomeron slope or a BFKL enhancement.

Our starting point is a very simple model that we published recently [5]. It is based on lowest-order perturbative QCD and on a very naïve approximation to the meson wave function [6], where in its rest frame the meson is simply described by two quarks at rest. Such an approximation should be valid provided that the meson motion is negligible, *i.e.* at very high Q^2. Despite its simplicity, this model was surprisingly successful and reproduced most of the features of the data: the mass dependence of the cross section came out naturally, as well as the Q^2 dependence. The model also predicted correctly s-channel helicity conservation, and even worked in photoproduction. It provided a test of two ideas: first of all, elastic production is mainly due to two gluons interacting with the meson, secondly, as the mesons were supposed to be made of their constituent quarks, the main production mechanism involves only the lowest Fock state.

Despite its many successes, this model failed, as most other, in the fact that the ratio σ_L/σ_T was predicted to be a factor 8 higher (at $Q^2 = 20$ GeV^2) than observed experimentally. As σ_L is much larger than σ_T, the high-Q^2 total cross sections $\sigma_L + \sigma_T$ were unaffected by this failure, but it is a strong indication that the model is far from complete. We want to emphasize that so far no model manages to reproduce the plateau observed experimentally, and that the best one has been able to do is to get a slower linear rise.

We shall show here that a re-consideration of the role of Fermi momentum enables one to preserve all the previous successful results while reproducing the ratio σ_L/σ_T. We keep the two fundamental assumptions of our previous paper, that the process is dominated by the coupling of two gluons to the lowest Fock state. In Section 2, we introduce the general formalism which we shall use for the description of the quarks contained in the meson. In sections 3 and 4, we give the general form of the amplitude. In section 5, we show that the amplitude is in general infrared finite, and in section 6 we give our results, and discuss the off-shell contribution to the amplitude. We then conclude, and pose several questions concerning the validity of the wave function formalism, and of the connection between diagonal and off-diagonal DIS tensors.

2 Vertices vs. wave functions

We shall assume here a form of factorisation, in that we shall not consider soft exchanges between the proton and the meson, but only concentrate on a hard scattering, a meson vertex function, a singlet exchange and a proton form factor. We do keep the exact kinematics, including transverse motion and quark masses, in the amplitude describing the transition $\gamma^* \to V$ as we want to assess the contribution of near-shell partons.

We need a model for the off-diagonal structure function, and we adopt the simplest one: at high energy, the process is dominated by pomeron exchange, which we model by two gluons times a Regge factor. The model of the off diagonal structure function will be obtained by convoluting the exchange with a proton form factor, which partially kills the infrared divergences.

The hard process generating the meson, and the $q\bar{q} \to V$ amplitude are treated together through the introduction of a meson vertex function. We shall make the assumption that the gluons couple to the constituent quarks of the meson, and assume that the direct coupling of gluons to the V vertex is negligible. In general, this is not the case, as the vertex must result from a non-perturbative resummation of diagrams involving quarks and gluons, to which perturbative gluons can in general couple directly. In fact, in all generality, such diagrams are needed to obtain a gauge invariant amplitude [7, 8]. However, as we shall see, these terms do not contribute in the high-energy limit.

Hence we are left with the description of the $\bar{q}qV$ vertex, and the gluons will couple to the quarks emerging from this vertex. In general, this vertex can depend on the 4-momenta respectively of the vector meson, of the quark, and of the antiquark, $V \equiv 2v$, $v + l$ and $v - l$, as well as on γ_μ. We know experimentally that vector-meson electroproduction conserves s-channel helicity, hence the only possible tensor structure is γ_μ. We are thus left with a vertex:

$$\Gamma_\mu = \Phi(l)\gamma_\mu \tag{1}$$

We shall assume that the vertex function Φ can depend only on the relative 4-momentum l, and that the dependence on the meson mass can be restated as a dependence on a Fermi momentum scale p_F.

This vertex function can be formally related [8] to a light-cone wavefunction, but we shall not make use of such a wavefunction in the meson case. Indeed, we find that the analytic structure of the propagator which is usually included in the definition of the wavefunction plays a crucial role in the reproduction of the ratio σ_L/σ_T. In the following, we shall make no further assumption concerning the quarks, except that we can treat them within perturbation theory. In particular, we shall not treat them *a priori* as on-shell particles.

In the following, we shall assume that the function Φ can be approximated for s states by a falling gaussian, multiplied by a normalisation constant N. As we do not assume that quarks are real particles, we do not have the usual wavefunction normalisation integral on Φ. However, the same vertex controls the decay $V \to e^+e^-$, and hence we shall be able to determine N so that it correctly reproduces the latter rate.

3 Calculation of the amplitude

3.1 Kinematics

The vectors of the problem are defined in Fig. 1. The photon has 4-momentum q and polarisation ϵ, with $q.q = -Q^2$. The vector meson has momentum $V = q+\Delta$ and polarisation e, with $t = \Delta^2$, $V^2 = m_V^2$, hence $\Delta.q = (m_V^2 - t + Q^2)/2$. The quarks composing the meson are written as $v + l$ and $-v + l$ with $v = V/2$.

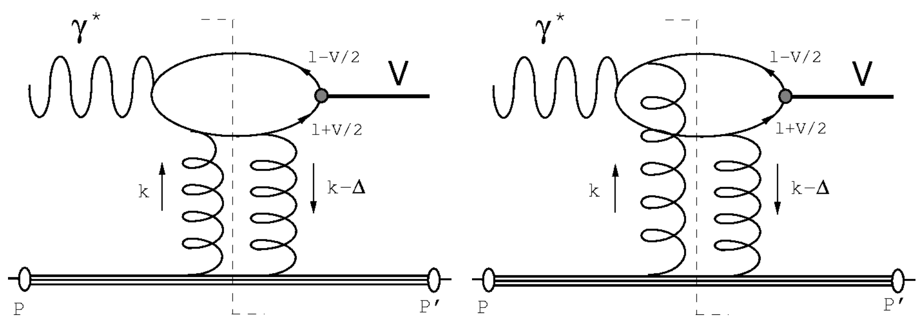

Figure 1: The two diagrams accounting for the transition $\gamma^* p \to V p$. The dashed line represents the cut which puts the intermediate state on-shell.

As we do not want to look in detail at the diffracted proton, we follow the usual treatment [9]: the momentum of the quark is p, and we assume that we can neglect its mass and put it on-shell $p.p = 0$. The fact that the proton quark remains on-shell after the scattering implies $p.\Delta = t/2$. We shall be working in the high-w^2 limit, and we write $p.q \approx (p + q)^2/2 \equiv \hat{w}^2/2$. We define $\hat{w} \approx w/3$ at the quark level, but this will not make any difference, as the final answer, in the large $\hat{w}$ limit, will be independent of $\hat{w}$.

3.2 The photon-meson bubble

Assuming that we can use perturbative quarks[†] in the upper bubbles, or equivalently that the non-perturbative effects can be reabsorbed into the vertex function, the upper bubbles of the graphs are described by the following traces:

$$\begin{aligned} T_1^{\alpha\beta} &= Tr\{\Phi(l)\ \gamma.e[\gamma.(v+l)+m_q]\gamma^\beta[\gamma.(q-v+l+k)+m_q]\gamma^\alpha \\ &\times\ [\gamma.(q-v+l)+m_q]\gamma.\epsilon[\gamma.(-v+l)+m_q]\} \qquad (2) \\ T_2^{\alpha\beta} &= Tr\{\Phi(l)\,\gamma.e[\gamma.(v-l)+m_q]\gamma^\alpha[\gamma.(v-k-l)+m_q]\gamma.\epsilon \\ &\times\ [\gamma.(v-q-k-l)+m_q]\gamma^\beta[\gamma.(-v-l)+m_q]\} \qquad (3) \end{aligned}$$

One of the quark lines connecting to the photon is off-shell and has different expressions in each diagram. Its propagator in the first graph is

$$P_1 = (q-v+l).(q-v+l) - m_q^2 = (l.l + 2l.q - 2l.v - 2q.v + \frac{m_V^2}{4} - m_q^2 - Q^2) \qquad (4)$$

whereas in the second graph it reads:

$$\begin{aligned} P_2 &= (-v+l+k).(-v+l+k) - m_q^2 \\ &= (k.k + 2k.l - 2k.v + l.l - 2l.v + \frac{m_V^2}{4} - m_q^2) \qquad (5) \end{aligned}$$

As we expect the amplitude to be w-independent, we shall be calculating the discontinuity of the amplitude, and the two intermediate quark propagators are put on-shell, which gives us the relations:

$$\begin{aligned} k.q &= \Delta.k + \Delta.q - k.k - 2k.l - 2l.q \qquad (6) \\ l.q &= -\Delta.l + l.l + m_V^2/4 - m_q^2 \qquad (7) \end{aligned}$$

One of the quarks constituting the meson is in general not cut, hence we have another propagator

$$P_5 = (v+l)^2 - m_q^2 = 2(l.l + m_V^2/4 - m_q^2) \qquad (8)$$

The sum of the two cut diagrams will then give:

$$T^{\alpha\beta} = [\frac{T_1^{\alpha\beta}}{P_1} + \frac{T_2^{\alpha\beta}}{P_2}]\frac{(2\pi)^2\delta(P_3)\delta(P_4)}{P_5} \qquad (9)$$

[†]One could easily extend this formalism and include non-perturbative effects present in the quark propagator, by replacing the quark mass m_q^2 by the parameters that enters in the Hilbert transform of the propagator, and by integrating over the Hilbert density afterwards. Such a complication is not needed to describe the data.

3.3 Current conservation

One of the consequences of gauge invariance is that the contraction of the upper bubble with the momenta of external lines is zero. In our case, we obtain indeed $k_\alpha T^{\alpha\beta} = 0$, and $T^{\alpha\beta}(\epsilon \to q) = 0$. However, we do not obtain exact current conservation for the off-shell quark emerging from the meson vertex: $(k-\Delta)_\beta T^{\alpha\beta} \sim l.v \neq 0$. In the photon case, one can recover explicit current conservation at the β vertex by crossing both sides of the diagram [10]. This can be accomplished by the substitution $T \to \frac{1}{2}[T(l) + T(l \to \Delta - k - l)]$. In our case, however, because of the presence of the vertex function, such substitution is not possible, and the current conservation that could be checked explicitly at the β vertex in the photon case is in general absent.

We can however impose that current conservation be satisfied, which amounts to putting the other quark making up the vector meson on-shell. The amplitude then splits into 2 physical processes: $\gamma gg \to \bar{q}q$ and $\bar{q}q \to V$. This of course leads to current conservation and ensures gauge invariance. This is the approach usually followed in a wave function formalism. It has the drawback of relying heavily on the existence of a mass shell for the quarks, and as we shall see does not lead to observed results.

However, we can pursue another route, by keeping the gauge dependence of the propagators, and checking explicitly that it cancels out in the large w^2 limit. As we shall see, the leading terms come from terms in which the momenta of the upper bubble get contracted with momenta of the lower quark lines. This means that terms proportional to $g_{\mu\nu}$ in the propagators are enhanced by a factor w^2 with respect to terms containing k_μ or k_ν, as the gluon momentum k will turn out to be transverse. Hence the large-w^2 limit is gauge invariant. We shall show explicitly that the infrared cancellation which is expected from gauge invariance occurs explicitly, albeit after integration over the photon-meson bubble.

3.4 The full amplitude

In order to obtain the full amplitude, we need to add the contribution of the proton lines, and the gluon propagators. We represent the proton by a constituent model, introducing the two following forms factors [5, 9]:

$$\mathcal{E}_1(t = \Delta^2) \approx \frac{(3.53 - 2.79t)}{(3.53 - t)(1 - t/0.71)^2} \tag{10}$$

when both gluons hit the same quark line (this is a fit to the measured Dirac elastic form factor), and

$$\mathcal{E}_2(k, k-\Delta) = \mathcal{E}_1(k^2 + (k-\Delta)^2 - c\, k \cdot (k-\Delta)) \tag{11}$$

if the gluons hit different quark lines, with $c \approx 1$ [11].
The prescription to go from the quark-level process to the proton-level process

is then to multiply the amplitude by the form factor $\mathcal{F}(k,\Delta) = 3(\mathcal{E}_1 - \mathcal{E}_2)$. The leading contribution of the lower quark line being $4p^\alpha p^\beta$, we obtain the following expression for the amplitude:

$$\begin{aligned}
\mathcal{A} &= \frac{2}{3}(4\pi\alpha_S)^2\ g_{elm}e_Q \\
&\times \int \frac{d^4l}{(2\pi)^4}\int\frac{d^4k}{(2\pi)^4}\mathcal{F}(k,\Delta)\ \frac{1}{\sqrt{3}}\Phi\,(l) \\
&\times \frac{[4(p_\alpha p_\beta)(g^{\alpha\tau}+\lambda\frac{k^\alpha k^\tau}{k.k})(g^{\beta\mu}+\lambda\frac{(k-\Delta)^\beta(k-\Delta)^\mu}{(k-\Delta).(k-\Delta)})T_{\tau\mu}]}{k^2(k-\Delta)^2}
\end{aligned} \tag{12}$$

where λ is the gauge parameter and $e_Q g_{elm} = e_Q\sqrt{4\pi\alpha_{elm}}$ the electromagnetic coupling of the different vector mesons: $e_Q = \frac{1}{\sqrt{2}}$ for the ρ, $-1/3$ for the ϕ and $2/3$ for the J/ψ.

4 The high-energy limit

To take the large-w^2 limit, we shall use Sudakov variables, rewrite the vectors of the problem in terms of p and q, and define the transverse direction, noted with a "t" subscript, as being orthogonal to both p and q.

We first write the expression for the polarisation vectors. The transverse photon polarisation is simply a unit vector in the transverse plane, whereas the transverse polarisation of the vector is slightly more complicated, as the transverse plane has been defined w.r.t. q. Solving $e.e = -1$, $e.v = 0$, $\epsilon.\epsilon = 1$ and $\epsilon.q = 0$, we obtain:

$$\epsilon_L = \frac{2Q}{w^2}p + \frac{1}{Q}q \tag{13}$$

$$\epsilon_T = \epsilon_t \tag{14}$$

$$e_L = \frac{\Delta_t}{m_V} + \frac{-m_V^2 + Q^2 - t}{m_V w^2}p + \frac{t + w^2}{m_V w^2}q \tag{15}$$

$$e_T = e_t - \frac{2\Delta_t.e_t}{w^2}p \tag{16}$$

Taking into account the on-shell conditions, we obtain the following expansions for the measures and the 4-vectors:

$$\begin{aligned}
&d^4\Delta\ \delta_+((p-\Delta)^2)\ \delta_+((q+\Delta)^2 - m_V^2) = \frac{1}{2w^2}\ d^2\Delta_t \\
&\Delta = \Delta_t + \frac{m_V^2 + Q^2 - t}{w^2}p + \frac{t}{w^2}q
\end{aligned} \tag{17}$$

$$d^4l\ \delta_+((v-l).(v-l) - m_q^2) = \frac{1}{8(1-\beta)}\ d\beta d^2l_t\ \theta(1-\beta)$$

$$
\begin{aligned}
l = & \frac{l_t}{2} + \frac{\beta}{2} q \\
& + \frac{(2\Delta_t - l_t).l_t + \beta((\beta-1)Q^2 + m_V^2 - t) - m_V^2 + \mu_q^2}{2(\beta-1)\ w^2} p
\end{aligned} \tag{18}
$$

with $\mu_q = 2m_q$.

$$
\begin{aligned}
& d^4k\ \delta_+((q - v + l + k)^2 - m_q^2)\ \delta_+((p-k)^2) = \frac{1}{4(\beta+1)\ w^2}\ d^2k_t\ \theta(1+\beta) \\
& k = \frac{k_t}{2} + \frac{k_t^2}{4w^2} q \\
& + \frac{2[(1-\beta^2)Q^2 - t + \mu_q^2 - l_t.(l_t - 2\Delta_t)] - k_t.(-k_t + 2l_t - 2\Delta_t)(1-\beta)}{2(1-\beta^2)w^2} p
\end{aligned} \tag{19}
$$

The propagators then become:

$$
\begin{aligned}
P_5 &= 2l^2 + \frac{m_V^2 - \mu_q^2}{2} \\
k^2 &= \frac{k_t^2}{4} \\
(k-\Delta)^2 &= -\Delta_t.k_t + \frac{k_t^2}{4} + t
\end{aligned} \tag{20}
$$

In the following, we shall write the integrated amplitude as:

$$
\begin{aligned}
\mathcal{A}_{(T,L)} &= \frac{2}{3}(4\pi\alpha_S)^2\ g_{elm} e_Q \\
&\times \int \frac{d^2k}{(2\pi)^2} \int \frac{d^4l}{(2\pi)^4} \\
&\times \mathcal{F}(k,\Delta)\ \frac{1}{\sqrt{3}} \Phi\,(l)\ \ \bar{A}_{(T,L)}
\end{aligned} \tag{21}
$$

The leading terms in w^2 for the two amplitudes $\bar{A}_{(T,L)}$ then become $\bar{A}_T = N_T/D$ and $\bar{A}_L = N_L/D$ with

$$
\begin{aligned}
D &= (2\beta\Delta_t.l_t - l_t.l_t + \mu_q^2 + (\beta^2-1)m_V^2 - t\beta^2) \\
&\times ((1-\beta^2)Q^2 + \mu_q^2 - t - (l_t + k_t - 2\Delta_t).(l_t + k_t)) \\
&\times ((1-\beta^2)Q^2 + (2\Delta_t - l_t).l_t + \mu_q^2 - t) \\
&\times (4\Delta_t.k_t + k_t.k_t - 4t)k_t.k_t
\end{aligned} \tag{22}
$$

$$
\begin{aligned}
N_L &= \frac{4(1-\beta^2)\ Q}{m_V}[m_V^2(\beta^2-1) + t\beta^2 - \mu_q^2 + l_t.(l_t - 2\beta\Delta_t)] \\
&\times k_t.(2l_t + k_t - 2\Delta_t)
\end{aligned} \tag{23}
$$

$$
\begin{aligned}
N_T &= 8\epsilon_{t\mu} e_{t\nu} \\
&\times \ \{[-\Delta_t^\mu \Delta_t^\nu (\beta+1)\beta + \Delta_t^\mu l_t^\nu \beta - l_t^\mu l_t^\nu (\beta+1) + l_t^\mu \Delta_t^\nu (\beta^2+\beta+1)] \\
&\qquad (k_t + 2l_t - 2\Delta_t).k_t(1-\beta) \\
&\quad +[-\beta \Delta_t^\mu k_t^\nu - k_t^\mu l_t^\nu \beta^2 + k_t^\mu \Delta_t^\nu \beta^3 + l_t^\mu k_t^\nu] \\
&\quad \times[t - \mu_q^2 - (1-\beta^2)Q^2 + l_t.l_t - 2\Delta_t.l_t] \\
&\quad -g^{\mu\nu}[-k_t.(k_t+l_t)(l_t.l_t - \mu_q^2) - (1-\beta^2)k_t.l_t Q^2 \\
&\qquad +\Delta_t.\Big((\mu_q^2 - l_t.l_t)(\beta-2)k_t + ((\beta+1)k_t.k_t + 2\beta k_t.l_t - 2\Delta_t.k_t)l_t\Big) \\
&\qquad +tk_t.(\Delta_t\beta - k_t\beta - 2l_t\beta + l_t) \\
&\qquad +(1-\beta^2)\beta\Delta_t.k_t Q^2]\} \qquad (24)
\end{aligned}
$$

In order to proceed further, we choose two orthogonal polarisation vectors in the transverse case, and there are a priory four transverse amplitudes, as the polarisation vector can each be taken parallel or orthogonal to a fixed direction. However, we find that the non diagonal terms, in which the photon and the vector meson have orthogonal polarisations, cancel in the angular integration. Hence in general we have only two diagonal transverse amplitudes to consider.

5 Properties of the amplitudes and of the cross section

To pursue analytically, we shall concentrate on the case $t = 0$ and $\Delta = (m_V^2 + Q^2)/w^2 p$. We shall give numerical results at all t further on. We can then perform the angular integrals analytically. In this case, the remaining two transverse amplitudes become equal after angular integration. Hence we are left with a transverse and longitudinal amplitudes, dA_L and dA_T, which we still need to integrate over β, $\mathbf{k_t}^2$ and $\mathbf{l_t}^2$. We use bold-faced letters to denote euclidian vectors in the transverse plane, hence $k_t^2 = -\mathbf{k_t}^2$, etc.

We cannot perform the $\mathbf{k_t}^2$ integral, as it depends on the proton form-factor. For the $\mathbf{l_t}^2$ integral, we change variable to l^2 as this is the variable entering the vertex function.

$$\mathbf{l_t}^2 = (1-\beta^2)m_V^2 - \mu_q^2 + 2(\beta-1)\mathcal{P} \qquad (25)$$

As we are going to discuss the real part and the imaginary part of the expression, we express the pole explicitly:

$$\mathcal{P} = 2l^2 + \frac{m_V^2 - \mu_q^2}{2} + i\epsilon \qquad (26)$$

Defining :

$$L^2 = (1-\beta^2)(Q^2+m_V^2) - 2(1-\beta)\mathcal{P}$$
$$M^2 = 2(1-\beta^2)m_V^2 - 2(1-\beta)\mathcal{P}$$
$$K^4 = (L^2+\mathbf{k_t}^2)^2 - 4\mathbf{l}_t^2\mathbf{k_t}^2$$

we obtain after angular integration:

$$dA_L = \frac{-(1-\beta^2)\ Q\ M^2(K^2-L^2)}{(2\pi)^3\ K^2\ L^2\mathbf{k_t}^4 m_V\ \mathcal{P}}\ dl^2\ d\beta\ d\mathbf{k_t}^2 \quad (27)$$

$$dA_T = \frac{-1}{(2\pi)^3\ K^2L^2\mathbf{k_t}^4\ 2\mathcal{P}}\ dl^2\ d\beta\ d\mathbf{k_t}^2 \\ \{(K^2-L^2)[(1+\beta^2)(L^2-2\mathbf{l_t}^2)-4\mu_q^2] - \mathbf{k_t}^2L^2(1+\beta^2)\ \} \quad (28)$$

The positive energy condition $(v-l).v > \frac{m_V\mu_q}{4}$ implies that

$$l^2 < \frac{(m_V-\mu_q)^2}{4} \quad (29)$$

These expressions have the following remarkable properties:
i) The small-$\mathbf{k_t}$ behaviour of both amplitudes is precisely $1/\mathbf{k_t}^2$. This is essential as it means that there is no IR singularity: the remaining divergence is handled by the proton form factor. We get:

$$dA_T(\mathbf{k_t}=0) = \frac{-2[(1+\beta^2)\mathbf{l_t}^2(\mathbf{l_t}^2-L^2)+\mu_q^2(2\mathbf{l_t}^2-L^2)]}{(2\pi)^3\ L^6\mathbf{k_t}^2\mathcal{P}}\ dl^2\ d\beta\ d\mathbf{k_t}^2 \quad (30)$$

$$dA_L(\mathbf{k_t}=0) = \frac{-(1-\beta^2)QM^2(L^2-2\mathbf{l_t}^2)}{(2\pi)^3\ L^6\mathbf{k_t}^2 m_V\mathcal{P}}\ dl^2\ d\beta\ d\mathbf{k_t}^2 \quad (31)$$

ii) One recovers the ratio A_L/A_T of our previous work, in the limit of zero Fermi momentum:

$$dA_T(\beta=0,\mathbf{l_t}=0) = \frac{2\mu_q^2 dl^2 d\beta d\mathbf{k_t}^2}{(2\pi)^3(Q^2+\mu_q^2+\mathbf{k_t}^2)(Q^2+\mu_q^2)\mathbf{k_t}^2\mathcal{P}} \quad (32)$$

$$dA_L(\beta=0,\mathbf{l_t}=0) = \frac{-\ Q\ (m_V^2+\mu_q^2)dl^2 d\beta d\mathbf{k_t}^2}{(2\pi)^3(Q^2+\mu_q^2+\mathbf{k_t}^2)(Q^2+\mu_q^2)m_V\mathbf{k_t}^2\mathcal{P}} \quad (33)$$

For $\mu_q^2 = m_V^2$ and $Q >> m_V$, we recover $|\frac{dA_L}{dA_T}| = \frac{Q}{m_V}$.
iii) There is no divergence at the edge of the β integrals. The longitudinal cross section is zero, and the transverse cross section goes to a constant, *independent of* Q^2.

$$dA_T(\beta=-1) = \frac{(K^2-L^2+\mathbf{k_t}^2)}{(2\pi)^3\ K^2\mathbf{k_t}^4\ \mathcal{P}}\ dl^2\ d\beta\ d\mathbf{k_t}^2 \quad (34)$$

$$dA_T(\beta=+1) = \frac{dl^2\ d\beta\ d\mathbf{k_t}^2}{(2\pi)^3\ \mathbf{k_t}^2\ \mathcal{P}} \times \left[\frac{1}{K^2} + \frac{(m_V^2-2Q^2-4l^2+\mu^2)}{\mathbf{k_t}^2(m_V^2+2Q^2-4l^2+\mu^2)}\right] \quad (35)$$

$$dA_L(\beta=\pm 1) = 0 \quad (36)$$

We can now perform the β integration. Taking into account condition (29), we write $l^2 = (m_V - \mu_q)^2/4 - \lambda^2$. The positivity of $\mathbf{l_t}^2$ from (25) constrains β to be contained between the bounds:

$$\beta_\pm = \frac{\pm 2\sqrt{\lambda^2 + \mu_q m_V}\lambda - 2\lambda^2 - \mu_q m_V + m_V^2}{m_V^2} \tag{37}$$

The lower bound of integration is always comfortably below 1 for nonzero μ_q and finite λ. The lower bound becomes smaller than -1, and is then not realised, for $\lambda > \sqrt{m_V^2 - m_q m_V}$.

However, the amplitude has a pole in l^2, or equivalently in λ^2, at

$$\mathcal{P} = 0 \Rightarrow l^2 = \frac{\mu_q^2 - m_V^2}{4} \tag{38}$$

hence we obtain a contribution from the principal part integration, and a contribution from the discontinuity. The latter corresponds to a direct extension of our previous model: both quarks constituting the meson are on-shell, and, after integrating over β, we obtain the following for the contribution to the amplitude at high Q^2:

$$dA_{L(disc)} \approx \frac{-8m_V\beta_d}{\mathbf{k_t}^2 Q^3} \frac{dl^2 d\mathbf{k_t}^2}{(2\pi)^3} \tag{39}$$

$$dA_{T(disc)} \approx \frac{-4m_V^2\beta_d + 2(\mu_q^2 + 2m_V^2)\log(\frac{1+\beta_d}{1-\beta_d})}{\mathbf{k_t}^2 Q^4} \frac{dl^2 d\mathbf{k_t}^2}{(2\pi)^3} \tag{40}$$

The bounds on β corresponding to (37) are $\beta_d^2 = \frac{m_V^2 - \mu_q^2}{m_V^2}$, far away from $\beta = \pm 1$. We see that the ratio dA_L/dA_T is still linear, but depends on the quark mass chosen. In the limit $\beta_d \to 0$, we of course recover our previous results for the ratio, and that the ratio Q/m_V gets multiplied by a constant, which depends on the quark mass. Unfortunately, this constant is always between 0.5 and 1, as shown in Fig. 2 for reasonable values of the (constituent) quark mass. Hence the discontinuity alone cannot solve the problem of the ratio σ_L/σ_T.

Note that it is possible to extend somewhat the previous expressions. Although the expressions include Fermi motion, they really single out a value of l^2 which corresponds to the on-shell condition, and the remaining β integral can be reduced to an angular integral in the meson center-of mass frame. One can make another model, where the quark mass is a priori not fixed, but a function of l^2, chosen so that the on-shell condition (38) is satisfied. The remaining integration involves then the vertex function $\Phi(l)$, and it cannot be done analytically. We have tried this route numerically, and find that the ratio remains linear, and can be somewhat reduced, by about a factor 2. This is not enough to reproduce the measured values, and is reminiscent of the situation encountered using a light-cone wavefunction formalism.

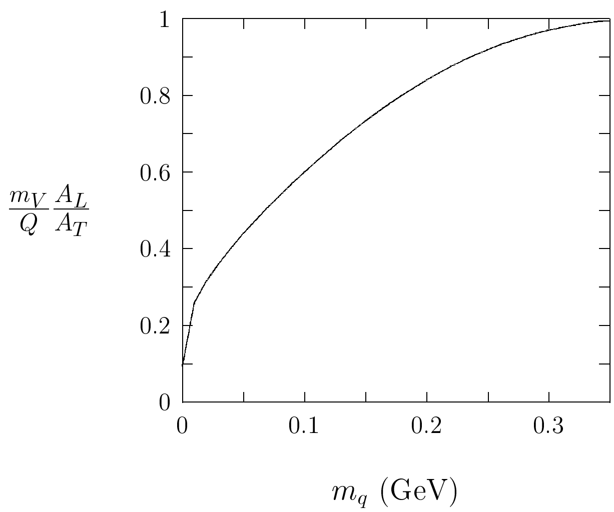

Figure 2: The reduction factor in the ratio σ_L/σ_T as a function of the quark mass

At this point, we still have not included the contribution of the principal part integration. This corresponds to letting one of the quarks off-shell, and there is no reason to neglect it. In fact, in the case of DIS, the kinematics is such that this is the only contribution. Its structure is somewhat different from that of the discontinuity. Indeed, the value of l^2 is not fixed anymore, hence the integration over β has only the bounds (37). In particular, once l^2 becomes large and negative, the value $\beta = -1$ can be realised. As we have mentioned in Eqs. (35), the transverse part retains a finite value there, whereas the longitudinal part goes to zero. Hence there is a narrow peak which gives a contribution only in the transverse case. If we include only the large λ contribution (the other parts turn out to be negligible), one obtains:

$$
\begin{aligned}
dA_{L(PP)} &= \frac{dl^2\ d\mathbf{k_t}^2}{(2\pi)^3\ \mathbf{k_t}^2\ m_V Q^3} \times \left\{ \frac{2m_V^2(1+\beta_+)}{\mathcal{P}} \right. \\
&+ \left. \log\left[\frac{(4\mathcal{P}-\mathbf{k_t}^2)\ \mathcal{P}}{(1+\beta_+)^2 Q^4}\right] - 4\frac{\mathcal{P}}{\mathbf{k_t}^2}\log\left[\frac{4\mathcal{P}-\mathbf{k_t}^2}{2\mathcal{P}}\right]\right\} \qquad (41)
\end{aligned}
$$

$$
dA_{T(PP)} = \frac{-2\ \log\left(\frac{4\mathcal{P}-\mathbf{k_t}^2}{4\mathcal{P}}\right)}{\mathbf{k_t}^4\ Q^2}\frac{dl^2\ d\mathbf{k_t}^2}{(2\pi)^3} \qquad (42)
$$

We can see that the real parts behave like $dA_L \propto \frac{1}{Q^3}$, and $dA_T \propto \frac{1}{Q^2}$ at high Q^2, plus logarithmic corrections, whereas the imaginary parts still behave like $dA_L \propto \frac{1}{Q^3}$, and $dA_T \propto \frac{1}{Q^4}$. Because this effect is present only at large λ, it is suppressed by the fall-off of the vertex function, and sets in only at relatively large Q^2. The leading behaviour of the principal parts integrals comes from quark off-shellnesses bigger than the constituent quark mass. Whereas in the massless case [3] an increase in the cross section can only come from extremely small off-shellnesses, we find that the dominant region in the massive case is shifted by the quark mass: the principal part integral cancels as long as one is very close to the pole, and the kinematics is such that this cancellation is not present anymore once the off-shellness is of the order of the quark mass.

Hence the source of the plateau observed at HERA is the interplay between the real part and the imaginary part of the cross section. Our model in fact predicts that asymptotically the transverse and the longitudinal cross sections first become equal, and that ultimately the process is dominated by the transverse cross section. This prediction is however driven by the details of the quark propagators, which could be modified by confinement effects.

6 Results

We shall now give our numerical results, which come from a numerical study of the full integrands at all t values. Before doing so, though, we shall need to define the vertex function, and to normalise it.

6.1 Vertex function and normalisation

The function Φ is unknown, and only its general analytical properties are well established [8]. In general, this function can depend on the scalar products $V.V$, $V.l$ and $l.l$. However, as in our case one of the quarks is on-shell, and as the meson is on-shell, only one of these scalar products is free. As in the case of the imaginary part, our results reduce to those of a wavefunction formalism, we shall assume that the vertex function is similar to the wavefunction of an s state. In the case of the ρ, the J/ψ and the ϕ, we take the form:

$$\Phi\left(l\right) = N\ e^{-\frac{\mathbf{L}^2}{2p_f^2}} \tag{43}$$

where $\mathbf{L}^2$ is the quark 3-momentum in the meson rest frame, equal to $\mathbf{L}^2 = (\frac{l.V}{m_V})^2 - l.l$, where the Fermi momentum p_F is 0.3 GeV in the ρ and ϕ cases, and 0.6 GeV in the J/ψ case [12], and where the quark masses are taken to be $m_{u,d} = 0.3$ GeV, $m_s = 0.45$ GeV and $m_c = 1.5$ GeV.

We can now fix the normalisation constant N by requiring that the decay rate $\Gamma \to e^+e^-$ be reproduced through the process depicted in Fig. 3.

The total decay rate, Γ, for $V \to f_1 f_2$ is given by:

$$\Gamma = \frac{1}{2m_V}\int \frac{d^4f_1 d^4f_2}{(2\pi)^2}|M|^2\delta^{(4)}(V - f_1 - f_2)\delta({f_1}^2 - {m_f}^2)\delta({f_2}^2 - {m_f}^2). \tag{44}$$

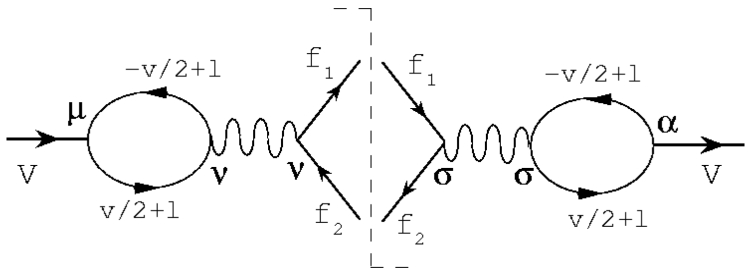

Figure 3: Diagram renormalising the vertex

with M the invariant amplitude corresponding to the diagram of Fig. 3:

$$\begin{aligned}
|M|^2 &= \int \frac{d^4l}{(2\pi)^4}\ T_1\ {g_{elm}}^2\ e_Q\ (\frac{3}{\sqrt{3}})\ \Phi\,(l) \\
&\times\ (T_2) \\
&\times\ \int \frac{d^4l'}{(2\pi)^4}\ T_3\ {g_{elm}}^2\ e_Q\ (\frac{3}{\sqrt{3}})\ \Phi\,(l) \\
&\times\ (\frac{1}{V^2})^2
\end{aligned} \tag{45}$$

With

$$T_1 = \frac{Tr[\gamma.e(\gamma.(-v+l)+m_q)\gamma^\nu(\gamma.(v+l)+m_q)]}{[(-v+l)^2-m_q^2][(v+l)^2-m_q^2]} \tag{46}$$

$$T_2 = Tr[\gamma^\nu(\gamma.f_2-m_f)\gamma^\mu(\gamma.f_1-m_f)] \tag{47}$$

$$T_3 = \frac{Tr[\gamma^\mu(\gamma.(-v+l)+m_q)\gamma.e(\gamma.(v+l)+m_q)]}{[(-v+l)^2-m_q^2][(v+l)^2-m_q^2]} \tag{48}$$

Putting the final leptons on-shell, neglecting their mass, working in the center-of-mass frame of the meson, where $l^2 = l_0^2 - \mathbf{L}^2$, and performing the angular integrals, leads to:

$$\begin{aligned}
\Gamma &= \frac{1}{2m_V}\ \frac{1}{(2\pi)^2}\ \frac{\pi V^2}{24}\ \frac{9}{3}\ {g_{elm}}^4\ {e_Q}^2\ (\frac{1}{V^2})^2\ (\frac{128}{3})^2 \\
&\times\ \Big[\int \frac{\mathbf{L}^2 dl_0 d\mathbf{L}}{(2\pi)^3}\ \frac{[3(4m_q^2+m_V^2)+4\mathbf{L}^2-12l_0^2]\ \Phi\,(l)}{(4l_0^2+4l_0m_V-4\mathbf{L}^2-4m_q^2+m_V^2+i\epsilon)}
\end{aligned}$$

$$\times \quad \frac{1}{(4l_0^2 - 4l_0 m_V - 4\mathbf{L}^2 - 4m_q^2 + m_V^2 + i\epsilon)} \Bigg]^2 \tag{49}$$

The integration over l_0 can be carried out by residues. We then get:

$$\begin{aligned} \Gamma &= \frac{1}{2m_V} \frac{2\pi}{3} {\alpha_{elm}}^2 {e_Q}^2 \frac{9}{3m_V^2} \left[\frac{8}{3(2\pi)^3} (2i\pi)^2 \right]^2 \\ &\times \left[\int \frac{\mathbf{L}^2 d\mathbf{L}}{\sqrt{\mathbf{L}^2 + m_q^2}} \frac{(2\mathbf{L}^2 + 3m_q^2)\ \Phi(l)}{(\mathbf{L}^2 + m_q^2 - \frac{m_V^2}{4})} \right]^2 \end{aligned} \tag{50}$$

The remaining integral over $\mathbf{L}$ still has a pole at the quark propagator. We must again keep both the discontinuity and the principal part of the integral. We in fact see that the phase of the amplitude becomes pure imaginary again once the vertex gets properly normalised. Introducing the function we have to deal with the pole in the denominator for $\mathbf{L} = \sqrt{\frac{m_V^2}{4} - m_q^2}$.
We introduce the notations:

$$\begin{aligned} z &= 2|\mathbf{L}| \\ z_d &= \sqrt{m_V^2 - \mu_q^2} \\ f(z) &= \frac{z^2}{\sqrt{z^2 + \mu_q^2}} \frac{(2z^2 + 3\mu_q^2)\ \Phi(z^2/4)}{(z - z_d)} \end{aligned} \tag{51}$$

with $\Phi(z^2/4) = N\ e^{\frac{-z^2}{8p_f^2}}$ then the integration over $\mathbf{L}$ gives:

$$\Gamma = \frac{4\alpha_{elm}^2\ {e_Q}^2}{9m_V^3\pi} \left[P \int_0^\infty \frac{f(z)dz}{z - z_d} + (i\pi)\ f(z_d) \right]^2 \tag{52}$$

It is worth pointing out that if we neglect the momentum l in the quarks loop, e.g. for $m_q = \frac{m_V}{2}$, we recover the formula [6] for the ρ meson:

$$\Gamma = \frac{f_m^2}{m_V} \frac{8\pi}{3} \alpha_{elm}^2\ e_Q^2 \tag{53}$$

We give in the Table the values of the decay rates [14] which we have fitted to, and the corresponding values of the normalisation N.

Meson	$\Gamma(V \to e^+e^-)$ (keV)	$\lvert N\rvert^2$	$p_F(GeV)$	m_q (GeV)
ρ	6.77	61.71	0.3	0.3
ϕ	1.37	72.01	0.3	0.45
J/ψ	5.26	44.91	0.6	1.5

Meson decay rates, vertex normalisation constants, Fermi momenta and quark masses.

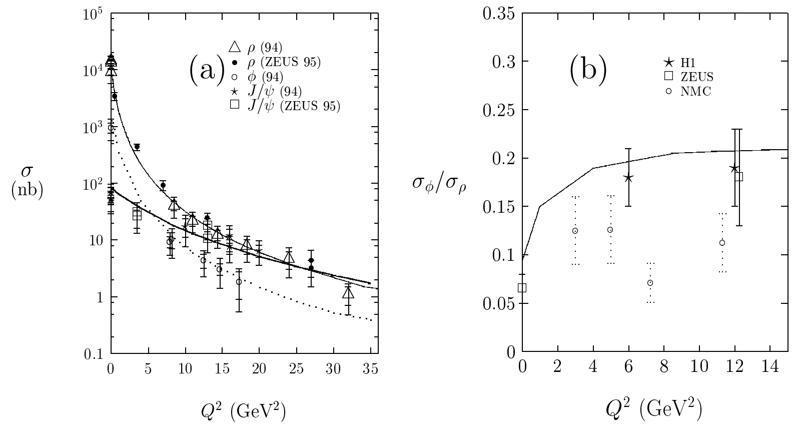

Figure 4: (a) Cross sections for ρ as functions of Q^2, compared with data from ZEUS [1] and H1 [2] at $< w > \approx 100$ GeV, (b) Ratio of cross sections as functions of Q^2 at $< w > \approx 100$ GeV, compared with data from H1 and Zeus [2, 1], and from NMC [13].

6.2 Q^2 and mass dependence of the cross section

The Q^2 behaviour of the total cross section, as well as the mass dependence, hardly get affected by the addition of Fermi momentum. This is because at low Q^2, the transverse amplitude is not modified by the addition of the real part, whereas at high Q^2 the cross section is still dominated by the longitudinal part at present values of Q^2. We show in Fig. 4.a the result of our model together with data from HERA. We have not corrected either for an eventual mass or Q^2 dependence of the Regge factor. Also, as our model does not include a prediction of the energy dependence, we have compared with 1994 data. New data are more precise, and allow one to observe that energy dependence directly from HERA data. The figure (plotted for data at $w^2 \approx 100$ GeV^2) shows however that the general features of the data are well reproduced: we see that a constant Regge factor (equal to 5.1) reproduces the data well for all mesons at HERA. This can be checked by considering figure 4.b which shows the ratio of cross sections, which goes well through the absolute predictions of our model. As in our previous model [5] we see that there seems to be a deficit of ϕ mesons w.r.t. ρ mesons at NMC, which we are unable to account for. Comparison with lower-energy data may lead to an estimate of α_S as well as of the intercept. These estimates are identical to those of [5] although the value of α_S should be multiplied by a factor $\sqrt{3}$ which we overlooked in our previous work [7]. It is again possible to go through the photoproduction point, although admittedly our model should not work for such low values of Q^2.

We have explained in great detail at $t = 0$ that ratio of the longitudinal and

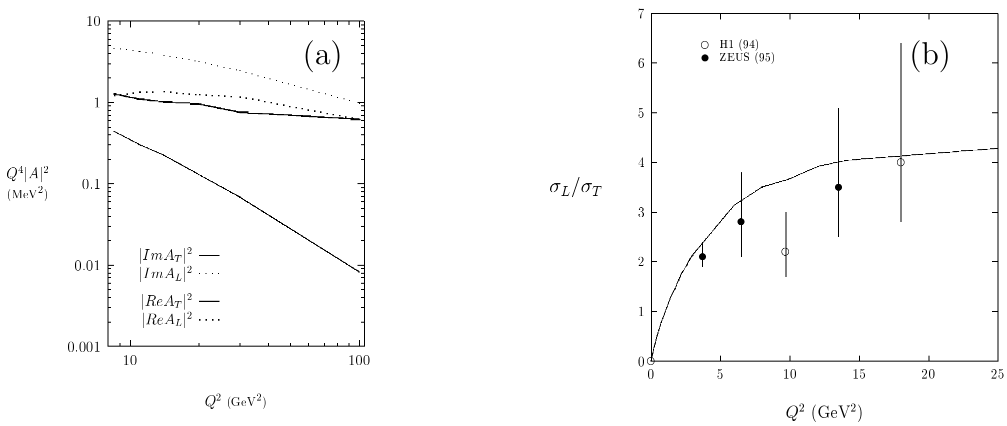

Figure 5: (a) Scaled behaviour of the real and imaginary parts of the transverse and longitudinal amplitudes, (b) Ratio of the longitudinal and transverse parts of the ρ cross section as functions of Q^2

transverse amplitudes has a plateau at large Q^2. It remains to be seen whether this feature is maintained for the t-integrated cross section. We show in Figure 5.a that this is indeed the case. Furthermore, as demonstrated in Fig. 5.b, for the values of Fermi momentum and for the quark masses shown in the Table, one falls right on top of the data. There is of course some uncertainty linked to these values, but a change of 50% in either leads to a change of about 20% in the ratio σ_L/σ_T.

6.3 Photoproduction, Regge factor and t dependence of the cross section

As we briefly mentioned, our model works in the deep non-perturbative region of photoproduction. It may be worth mentioning at this point that even at large values of Q^2 the gluon off-shellnesses are not large, and as we have seen quark off-shellnesses must be near m_q in the real part. Hence the situation is not dramatically different in the case of photoproduction, but nevertheless, it still comes as a surprise that the model applies in this region. This may hint at a lower-Q^2 generalisation of the factorisation theorem.

We show in Fig. 6.a the ρ photoproduction cross section $d\sigma/dt$ and compare it with our model. We see that we obtain excellent agreement, although our curve is not an exponential. In Fig. 6.b, we show the Q^2 dependence of the b slopes from our model: the experimental points correspond to a fit to Ne^{bt}, and our curve corresponds to $1/< t >$, which would be the same were the curve an exponential. We see that despite the curvature of our curves, the agreement is quite good. The

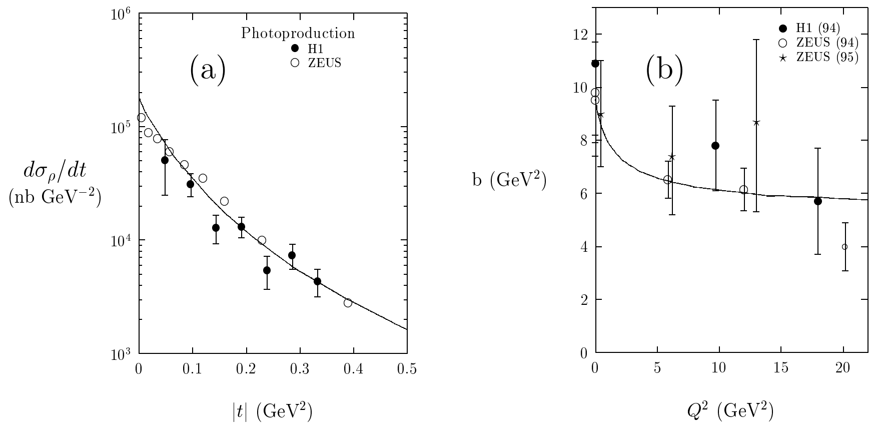

Figure 6: (a) Differential cross section $d\sigma/dt$ for elastic ρ^0 photoproduction, compared with HERA data [1, 2], (b) t-slope of the photoproduction differential elastic cross sections, compared with HERA data [1, 2].

t-dependence of other mesonic cross sections is predicted in Fig. 7. Comparison with preliminary "public" data from ZEUS [15] would indicate good agreement. We trust that the forthcoming ZEUS published analysis will confirm this result. Hence, if we believe this model is applicable to photoproduction, we see there is little room either for a BFKL large t enhancement or for a pomeron slope.

6.4 Predictions for ρ' and Ψ'

Given the success of our model in reproducing the lowest mass vector mesons, we can easily extend it to study the 2s excited states. The first ingredient is the vertex function, which we take as:

$$\Phi_{2s} = N\sqrt{2/3}\left(-\frac{3}{2} + \frac{\mathbf{L}^2}{p_F^2}\right)\exp\left(-\frac{\mathbf{L}^2}{2p_F^2}\right) \tag{54}$$

with $\mathbf{L}$ as defined below Eq. (43), and the values of p_F and m_q the same as in the 1s case. The normalisation constant N should again be determined from the leptonic decay of the vector meson. The latter is available only in the ψ' case [14], hence we can make predictions only in this case: $\gamma(\psi' \to e^+e^-) = 5.26$ keV leads to $N = 35.36$. The ratio of the ψ' elastic production to that of the J/ψ, at low $Q^2 < 0.01$ GeV^2 is calculated to be 0.165, in excellent agreement with the H1 measurement [16], as can be seen from Fig. 8.a.

In the ρ' case, we can calculate N from the elastic production and make predictions for the leptonic width: from the preliminary "public" results of the H1 collaboration [17], which we were unfortunately asked not to quote [18], we

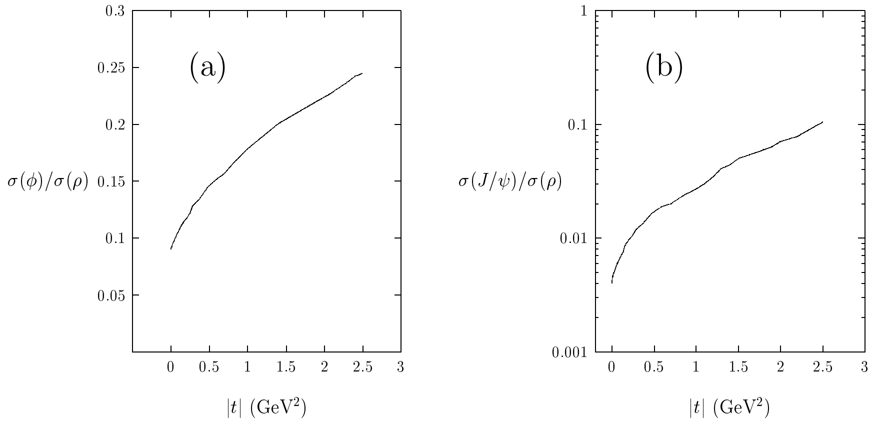

Figure 7: Ratio of the differential photoproduction cross sections for (a) ϕ and ρ mesons and (b) for J/ψ and ρ mesons.

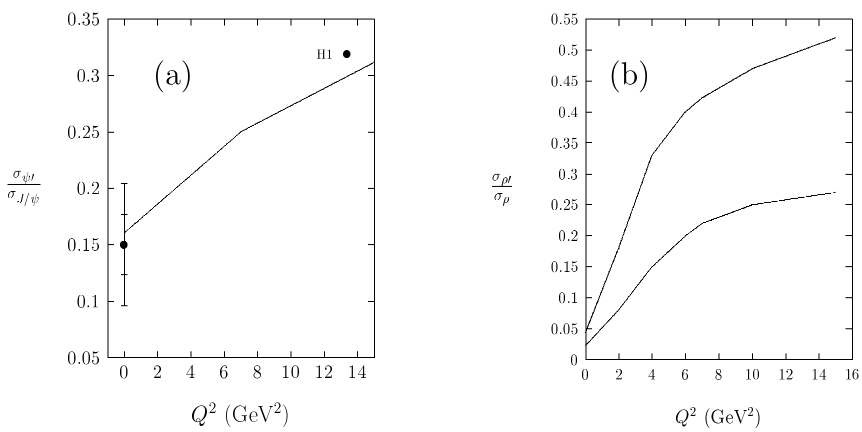

Figure 8: (a) Prediction for the ratio of the ψ' production cross section to that of the J/ψ, compared with H1 data [16] (b) prediction for the ρ' cross section based on the consideration of H1 preliminary "public" data [17], leading to the prediction of the leptonic width (55).

obtain

$$\Gamma(\rho' \to e^+e^-) = 1.1 \pm 0.34 \text{ keV} \tag{55}$$

The resulting predictions are shown in Fig. 8.b. We see that although the normalisation of this figure is not predicted, the ratio is predicted to increase sharply with Q^2 and hence an eventual final measurement at HERA should find a substantially higher cross section than the one at fixed target experiments.

7 Conclusion

We have presented here a model which reproduces all the features (except the w^2 dependence) of elastic vector meson production as observed at HERA. Although the model is built to work at large values of Q^2, it extends to the nonperturbative photoproduction region. The main result is that it is possible to reproduce the ratio σ_L/σ_T. The plateau observed experimentally comes from the interplay between the on-shell and the off-shell quark contributions, which have different asymptotic behaviours. Hence it is essential to allow quarks to be virtual, as in the standard DIS case.

It is worth pointing out that despite its successes, our model has not been tuned to reproduce the data: the values of the Fermi momentum, the form of the wavefunction and the quark masses are given in the Table, and are only reasonable guesses. Similarly, the proton form factor could be modified, as it is known only in the IR limit. We find remarkable that educated guesses lead to such a good agreement with data.

Hence it is essential to allow quarks to be off-shell not only to reproduce the behaviour of the transverse part, but also because the relation to structure functions is only possible then. Indeed, the $\log Q^2$ terms of Eq. (41) are the same as those of the upper quark loop in DIS. The use of wavefunctions can miss such contributions, as they come from a part of the amplitude which is usually embedded in the wavefunction.

Note

A previous version of this paper showed preliminary H1 and ZEUS data scanned from "public" documents available from the web and comparing them with our model. Although we found beautiful agreement, the H1 collaboration demanded that we remove these from the published version, and the ZEUS collaboration indicated that they as well do not want preliminary results included for comparison in theoretical papers. We have thus removed these data, and deeply regret to have taken the scientific liberty of explaining experimental results publicly available before they are published. We want to indicate that that policy should be spelled out explicitly in the papers and in the webpages available, as comparing results with (even unpublished) data is -and should be- a common trend among theorists.

Acknowledgments

We thank Markus Diehl for several essential discussions, and for correcting some of our formulae, Roberto Sacchi (Zeus) for giving us the files connected with his analyses of the data, J. Gravelis and A. Donnachie for spotting a mistake in an earlier version of this paper, Barbara Clerbaux for making us aware of the rules of the H1 collaboration concerning preliminary data, and Bruno Van Den Bossche for sharing his knowledge of meson wave functions with us.

References

[1] ZEUS collaboration, J.Breitweg et al., preprint DESY 98-107 (August 1998), submitted to *Eur. Phys. J.*; M. Derrick et al., *Eur. Phys. J.* **C2** (1998) 247; *Z. Phys.* **C73** (1997) 253; *Phys. Lett.* **B380** (1996) 220; *Phys. Lett.* **B377** (1996) 259; *Phys. Lett.* **B356** (1995) 601; *Phys. Lett.* **B350** (1995) 120; *Z. Phys.* **C69** (1995) 39.

[2] H1 collaboration, C. Adloff et al., *Phys. Lett.* **B421** (1998) 385; S. Aid et al., *Z. Phys.* **C75** (1997) 607; *Nucl. Phys.* **B472** (1996) 3; *Nucl. Phys.* **B468** (1996) 3; *Nucl. Phys.* **B463** (1996) 3. T. Ahmed et al., *Phys. Lett.* **B338** (1994) 507.

[3] John C. Collins, Leonid Frankfurt, and Mark Strikman, *Phys. Rev.* **D56** (1997) 2982.

[4] See *e.g.* V.S. Fadin and L.N. Lipatov, preprint DESY-98-033 (Feb 1998), e-Print Archive: hep-ph/9802290; Marcello Ciafaloni and Gianni Camici, preprint DFF-302-03-98 (March 1998), e-Print Archive: hep-ph/9803389; D.A. Ross, preprint SHEP-98-06 (Apr. 1998), e-Print Archive: hep-ph/9804332; Yuri V. Kovchegov and A.H. Mueller, preprint CU-TP-889 (May 1998), e-Print Archive: hep-ph/9805208; and references therein.

[5] J.R. Cudell and I. Royen *Phys. Lett.* **B397** (1997) 317; e-Print Archive: hep-ph/9609490.

[6] A. Donnachie, R.R. Horgan, P.V. Landshoff, *Z. Phys.* **C10** (1981) 71 and *Phys. Lett.* **107B** (1981) 385; R.R. Horgan, P.V. Landshoff, D.M. Scott, *Phys. Lett.* **110B** (1982) 493.

[7] We thank M. Diehl for pointing this fact to one of us.

[8] A. Hebecker and P.V. Landshoff, *Phys. Lett.* **B419** (1998) 393; e-Print Archive: hep-ph/9710296, and talk given at 33rd Rencontres de Moriond: QCD and High Energy Hadronic Interactions, Les Arcs, France, 21-28 Mar 1998, e-Print Archive: hep-ph/9805321.

[9] J.F. Gunion and D. Soper, *Phys. Rev.* **D12** (1975) 163;

[10] J.R. Cudell, A. Donnachie and P.V. Landshoff, *Nucl. Phys.* **B322** (1989) 55.

[11] J.R. Cudell and O.F. Hernández, *Nucl. Phys.* **B471** (1996) 471.

[12] see e.g. H. G. Dosch, T. Gousset, G. Kulzinger, and H. J. Pirner, *Phys. Rev.* **D55** (1997) 2602.

[13] A. Sandacz, preprint SINS-9-VI (April 1995); NMC, M. Arneodo et al., Phys. Lett. **B332** (1994) 195-200; A. Sandacz et al., Nucl. Phys. **B429** (1994) 503-529.

[14] Particle Data Group, L. Montanet et al., *Phys. Rev.* **D50** (1994) 1173.

[15] J.A. Crittenden, contribution to the proceedings of the LISHEP International School on High-Energy Physics, Rio de Janeiro, Brazil, 16-20 February 1998, hep-ex/9806020.

[16] H1 Collaboration, C. Adloff et al., *Phys. Lett.* **B421** (1998) 385, e-Print Archive: hep-ex/9711012.

[17] J. Gayler (H1 collaboration), contribution to ICHEP96, 28th International Conference on High Energy Physics, Warsaw, Poland, July 1996, http://www-h1.desy.de/psfiles/proceedings/warsaw-96jg.ps.

[18] John Dainton, private communication.